PHYSICAL REVIEW A VOLUME 57, NUMBER 2 FEBRUARY 1998

Relativistic dielectronic recombination process: Electron and H-like ions

Yi-Zhi Qu,[1] Jian-Guo Wang,[2] Jian-Kui Yuan,[1] and Jia-Ming Li[1,3]
[1]*Institute of Physics, Chinese Academy of Sciences, P. O. Box 603, Beijing 100080, China*
[2]*Institute of Applied Physics and Computational Mathematics, P. O. Box 8009, Beijing 100088, China*
[3]*Department of Physics, Center of Atomic and Molecular Sciences, Tsinghua University, Beijing 100084, China*

(Received 14 July 1997)

We have developed a simplified relativistic configuration-interaction method to calculate the dielectronic recombination (DR) cross sections and rate coefficients. In this method, the infinite resonant doubly excited states can be treated conveniently in the framework of quantum defect theory. Here we report a systematic study of DR rate coefficients of hydrogenlike isoelectronic sequence with atomic number $2 \leqslant Z \leqslant 79$. The behavior of the DR rate coefficients along the isoelectronic sequence is studied. The results are compared with the Burgess formula and other theoretical works. Because of its relativistic treatment, our method can be applicable for arbitrary Z ions and the validity of the widely used Burgess formula can be examined, e.g., for the ion with $Z \geqslant 36$, the results calculated from Burgess formula would be larger by a factor of 2.
[S1050-2947(98)01902-7]

PACS number(s): 34.80.Lx, 34.80.Kw, 34.80.Dp

I. INTRODUCTION

Dielectronic recombination (DR) can be regarded as a resonant radiative recombination process. As a free electron with a specific kinetic energy collides with an ion A^{q+}, one of the bound electrons of the ion A^{q+} is excited from the initial $n_i l_i$ orbital into the NL orbital, the free electron is then captured into an unoccupied orbital nl and forms a resonant doubly excited state; subsequently, the resonant doubly excited state decays into a nonautoionizing state through radiative transition processes. Its importance in influencing the ionic balance in high-temperature plasmas, such as a solar corona, has been known for many years [1]. Its radiative emission is a significant contributor to plasma cooling in hot plasmas in fusion experiments. The dielectronic satellites of hydrogenlike ions have also been used to measure plasma densities in high-density plasmas [2] and the electron temperatures in solar flares [3].

Many theoretical methods have been developed to calculate the DR process, such as the distorted wave method [4,5], close-coupling methods [6,7], and nonrelativistic single configuration [8,9] and relativistic multiconfiguration methods [10,11]. In these calculations, it is tedious work to obtain the accurate DR rate coefficients since they involve many resonant doubly excited states. Most calculations either neglect high-lying doubly excited states or simply use the n^{-3} law to treat them [9,12,31,33]. In many applied aspects, such as astrophysics and plasma physics, the Burgess formula [13] is widely used for its convenience [14]. Based on quantum defect theory (QDT), we have developed a simplified relativistic configuration interaction (SRCI) method [15] and have calculated the DR cross sections of hydrogenlike helium [16] and argon [17]. Our theoretical results are in good agreement with the absolute cross-section measurements [18,19] within 10%. In this paper, we report a systematic study of DR rate coefficients of the hydrogenlike isoelectronic sequence. The calculations cover the ions with atomic number $2 \leqslant Z \leqslant 79$. The behavior of the DR rate coefficients along the isoelectronic sequence is studied. Because of its relativistic treatment, our SRCI method is applicable for arbitrary Z ions and then the validity of the Burgess formula [13] can be examined, e.g., for the ions with $Z \geqslant 36$, the results calculated from Burgess formula would be larger by a factor of 2.

II. THEORETICAL METHOD

The DR process of A^{q+} has the form

$$e^- + A^{q+}(n_i l_i) \rightarrow A^{(q-1)+}(NLnl)^{**} \rightarrow A^{(q-1)+}(1s n_k l_k)^* + h\nu, \tag{1}$$

where the A^{q+} ion in the initial state $i(n_i l_i)$ captures a free electron with a specific energy ϵ_i and forms the $A^{(q-1)+}$ ion in the resonant doubly excited state $j(NLnl)$. The cross sections of this resonant capture processes can be treated in the isolated resonance approximation

$$\sigma_{ij}^{c} = \frac{\pi^2 \hbar^3}{m_e \epsilon_i} \frac{g_j}{2 g_i} A_{ji}^{a} \delta(\epsilon - \epsilon_i), \tag{2}$$

where g_i and g_j are the statistical weight of the state i and j, respectively. A_{ji}^{a} is the Auger decay rate (inverse resonant capture process), which can be calculated by Fermi's "golden rule,"

$$A_{ji}^{a} = \frac{2\pi}{\hbar} \left| \langle \Psi_j | \sum_{s<t} \frac{1}{r_{s,t}} | \Psi_{i\epsilon_i} \rangle \right|^2, \tag{3}$$

where Ψ_j and $\Psi_{i\epsilon_i}$ are antisymmetrized many-electron wave functions for the j state and i state plus a free electron, respectively.

We construct the configuration wave functions $\phi(\Gamma JM)$ (Γ denotes the quantum numbers $NLnl$ and parity) as antisymmetrized product-type wave functions from central-field Dirac orbitals with appropriate angular momentum coupling [20]. All relativistic single-electron wave functions (bound and continuum) are calculated based on the atomic self-consistent potential obtained from the ground-state configuration for $A^{(q-1)+}$ [21,22]. In our SRCI method, the atomic-state function for the state $j(NLnl)$ with total angular momentum JM is expressed as a linear expansion of the configuration wave functions $\phi(\Gamma_\lambda JM)$ with the same principal quantum numbers (N,n), and the same orbital angular momentum quantum numbers (L,l):

$$\Psi_j(JM)=\sum_{\lambda=1}^{m} C_{j\lambda}\phi(\Gamma_\lambda JM). \tag{4}$$

Here m is the number of configuration wave functions; the mixing coefficients $C_{j\lambda}$ for state j are obtained by diagonalizing the relevant Hamiltonian matrixes [20]. We neglect the configuration interaction between the bound state and the continuum state and the state including a free electron is chosen as the single configuration wave function. Then we have

$$A^a_{ji}=\frac{2\pi}{\hbar}\left|\sum_{\lambda=1}^{m} C_{j\lambda}M^a_{ij\lambda}\right|^2, \tag{5}$$

where the Auger decay matrix element $M^a_{ij\lambda}$ is defined as

$$M^a_{ij\lambda}=\langle\phi(\Gamma_\lambda JM)|\sum_{s<t}\frac{1}{r_{s,t}}|\Psi_{i\epsilon_i}\rangle. \tag{6}$$

Based on QDT, when (N,L,l) are fixed and n varies from bound to continuum state, all the resonant doubly excited states with the same J will form a channel. In the channel, the energy-normalized matrix element can be defined as

$$\overline{M^a_{ij\lambda}}=M^a_{ij\lambda}(\nu_n^{3/2}/q), \tag{7}$$

where (ν_n^3/q^2) is the density of state, $\nu_n=n-\mu_n$, and μ_n is the corresponding quantum defect. This energy-normalized matrix element $\overline{M^a_{ij\lambda}}$ varies smoothly with the electron orbital energy in the channel [15,16]. When $\overline{M^a_{ij\lambda}}$ of a few states (including one continuum state) in a channel have been calculated, the Auger decay matrix elements of infinite discrete states of that channel can be obtained by interpolation. On the other hand, the mixing coefficients $C_{j\lambda}$ in Eq. (4) are almost unchanged for the states with large n within a channel [16]. We can use the mixing coefficients of a state with a certain high principal quantum number n to approximate that of those states with higher principal quantum number. From the expression (5), the Auger rates and capture rates (by detailed balance) of the infinite resonant doubly excited states can be obtained conveniently.

The resonant doubly excited state may autoionize with a rate A^a_{ji} by emitting an Auger electron or decay radiately into a lower energy state k with a radiative rate A^r_{jk}, which is defined as

$$A^r_{jk}=\frac{4e^2\omega}{3\hbar c^3 g_j}|\langle\Psi_j|T^{(1)}|\Psi_k\rangle|^2, \tag{8}$$

where ω is photon energy, and $T^{(1)}$ is the electronic dipole operator [16]. Similar to the expression (4), the atomic wave function Ψ_k for the final state k can be constructed as

$$\Psi_k(J'M')=\sum_{\lambda'=1}^{m'} C_{k\lambda'}\phi'(\Gamma'_\lambda J'M'). \tag{9}$$

Then we have

$$A^r_{jk}=\frac{4e^2\omega}{3\hbar c^3 g_j}\left|\sum_{\lambda,\lambda'=1}^{m,m'} C_{j\lambda}C_{k\lambda'}M^r_{jk}\right|^2, \tag{10}$$

where the radiative transition matrix element is defined as

$$M^r_{jk}=\langle\phi(\Gamma_\lambda JM)|T^{(1)}|\phi'(\Gamma'_\lambda J'M')\rangle. \tag{11}$$

For the radiative process with a certain final state k, the resonant doubly excited states with the fixed (N,L,l) and different orbital energy form a channel. In the channel, the energy-normalized radiative transition matrix element is defined as

$$\overline{M^r_{jk}}=M^r_{jk}(\nu_n^{3/2}/q). \tag{12}$$

This energy-normalized matrix element $\overline{M^r_{jk}}$ varies slowly with the electron orbital energy [16,23,24]. When $\overline{M^r_{jk}}$ of a few states (including one continuum state) in a channel have been calculated as benchmark points, all the energy-normalized matrix elements $\overline{M^r_{jk}}$ of infinite discrete states in that channel can be obtained by interpolation [23,24]. From expression (10), we can obtain all the radiative rates in the channel. For a certain initial state, the energy-normalized transition matrix element may have nodes, at which the matrix element is equal to zero [25]. In this case, the interpolation should be carried out for the energy-normalized transition elements and not for the radiative rates (i.e., proportional to the square of the transition elements).

The resonance energy ϵ_i can be calculated under the frozen-core approximation [26]. Specifically, we can calculate the energy $E(NLnl)$ of $A^{(q-1)+}$ and $E(NL)$ of core A^{q+} using the same bases under SRCI method. Then,

$$\epsilon_i=\Delta E^H(NL)+[E(NLnl)-E(NL)], \tag{13}$$

where the energy difference between $1s$ and NL for hydrogenlike A^{q+} can be calculated analytically, i.e., $\Delta E^H(NL)=Z^2[1/2-1/(2N^2)]$ (hartree).

We can then obtain the DR cross sections for any resonant doubly excited states conveniently,

$$\sigma_{ij;k}=\frac{\pi^2\hbar^3}{m_e\epsilon_i}\frac{g_j}{2g_i}\frac{A^a_{ji}A^r_{jk}}{\Sigma_{k'}A^r_{jk'}+\Sigma_{i'}A^a_{ji'}}\delta(\epsilon-\epsilon_i). \tag{14}$$

Here the summation i' is over all possible states of the A^{q+} ion, and the summation k' is over all possible states of $A^{(q-1)+}$ whose energies are below state $j(NLnl)$.

We assume that the velocity distribution of the free electron is the Maxwell-Boltzmann distribution, then the dielectronic recombination rate coefficients can be expressed as

$$\alpha_{ij;k}=\left(\frac{2\pi\hbar^2}{m_e\kappa T}\right)^{3/2}e^{-\epsilon_i/\kappa T}\frac{g_j}{2g_i}\frac{A^a_{ji}A^r_{jk}}{\Sigma_{k'}A^r_{jk'}+\Sigma_{i'}A^a_{ji'}}, \tag{15}$$

where T is the temperature of the electron and κ is Boltzmann's constant. And the total dielectronic recombination rate coefficients can be expressed as

$$\alpha^{\mathrm{DR}}=\sum_{j,k} \alpha_{ij;k}. \tag{16}$$

III. RESULT AND DISCUSSION

There are enormous intermediate resonance states involved in the DR process, which makes explicit calculations not practicable [27]. Hence, the n^{-3} scaling law is widely used in the literature to extrapolate the satellite intensity factors (proportional to DR cross section) for higher ($n \geqslant 4$) resonances [9,12,31,33]. Based on QDT, we have developed the SRCI method, in which all the high-lying resonant doubly excited states are treated conveniently through interpolation. When the energy-normalized matrix elements $\overline{M}^{a}_{ij\lambda}$ and $\overline{M}^{r}_{jk}$ of a few states (including one continue state) are calculated as benchmark points, all the Auger and radiative matrix elements and the corresponding rates of the infinite resonant doubly excited states can be obtained by interpolation with adequate accuracy and much less computational effort. In our calculation all the doubly excited states $NLnl$ with high n can be conveniently calculated based on QDT. Then, all the Coster-Kronig transitions (e.g., $2p_{3/2}nl \rightarrow 2p_{1/2}+e$) that become energetically possible for a certain high n are included in our calculation. We have calculated the DR cross sections for $\mathrm{He}^{+}(Z=2)$ [16] and $\mathrm{Ar}^{17+}(Z=18)$ [17], which are in good agreement with the recent absolute cross-section measurements [18,19] within 10%. For He^{+}, the electron-electron correlations (configuration interactions) are most important along the H-like isoelectronic sequence. The agreement shows that our SRCI method includes the main part of configuration interactions, i.e., the configuration interactions among the states with the same $NLnl$. The other configuration interactions of states with different $N'L'n'l'$ may affect the individual transition probabilities A^{a} and A^{r}. Anyhow, neglecting the other configuration interactions is anticipated to have an effect of a few percent on the total cross sections and rate coefficients since there is an agreement between the SRCI calculation results and the absolute cross-section measurements. This is owing to that ‘‘the errors and variations due to approximations introduced in the evaluation of the individual transition probabilities A^{a} and A^{r} tend to cancel,’’ as discussed in Ref. [34]. Furthermore, the configuration interactions, including interchannel interactions, which will be discussed in the next paragraph, only result in the redistribution of DR cross section among intermediate states. The SRCI method can be applied for arbitrary Z ions because of its relativistic treatment. We here report a systematic study of the total DR rate coefficients α^{DR} of hydrogenlike isoelectronic sequence with atomic number $2 \leqslant Z \leqslant 79$ using our SRCI method, as shown in Fig. 1 (solid curves). The results from the widely used Burgess formula [13] are also plotted in Fig. 1 (dotted curves). It is obvious, for the ion with $Z \geqslant 36$, that the results calculated from the Burgess formula would be larger by a factor of 2. As Z increases, the peaks of the DR rate coefficients $\alpha^{\mathrm{DR}}_{\max}$ as a function of T shift from low T to high T, while $\alpha^{\mathrm{DR}}_{\max}$ increase from $Z=2$ to $Z=4$ and then decrease.

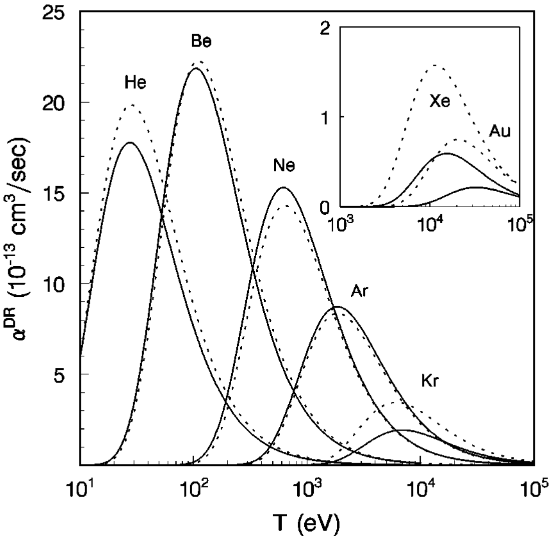

FIG. 1. The total DR rate coefficients α^{DR} vs temperature T. Solid curve: present calculation; dotted curve: Burgess formula.

The N dependence of the DR rate coefficients for He^{+} and Ne^{9+} ions are displayed in Fig. 2. The ratio of the partial DR rate coefficients of $3Lnl$ intermediate states to the $2Lnl$ partial DR rate coefficients is about 0.14 for He^{+}. It decreases rapidly with the increase of Z, e.g., only about 0.06 and 0.04 for Ne^{9+} and Ar^{17+}, respectively. Thus, the contribution of high N ($N \geqslant 3$) double excited states is less important, especially for the intermediate-Z and high-Z ions. Even for low-Z ions, we only need to consider the $2Lnl$ and $3Lnl$ contribution to the total DR rate coefficients. In our present SRCI calculation, the interchannel interaction is neglected. Thus, the calculated DR cross sections of the specific $3Lnl$ intermediate states for He^{+} are smaller than the experimental measurement [28]. Nevertheless, this will not affect our calculated total DR rate coefficients, since the interchannel interaction only result in the redistribution of the DR cross section among $2Lnl$ and $3Lnl$ intermediate states, which will be discussed elsewhere [29].

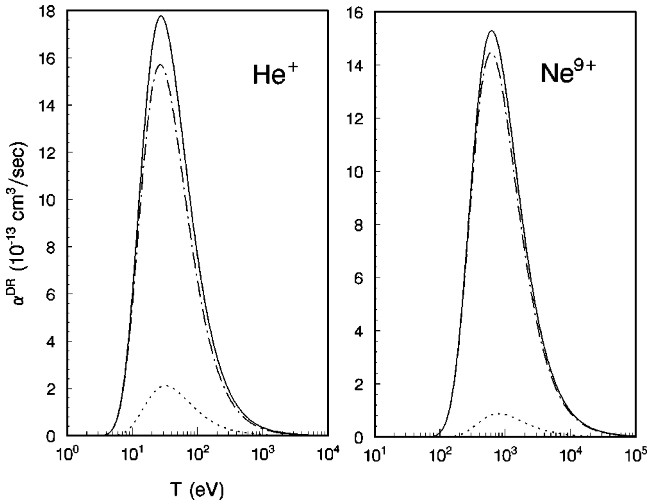

FIG. 2. The contribution of $2Lnl$ and $3Lnl$ intermediate states to the DR rate coefficients for He^{+} and Ne^{9+} ions. Solid curve: total DR cross section; dot-dashed curve: $2Lnl$; dotted curve: $3Lnl$.

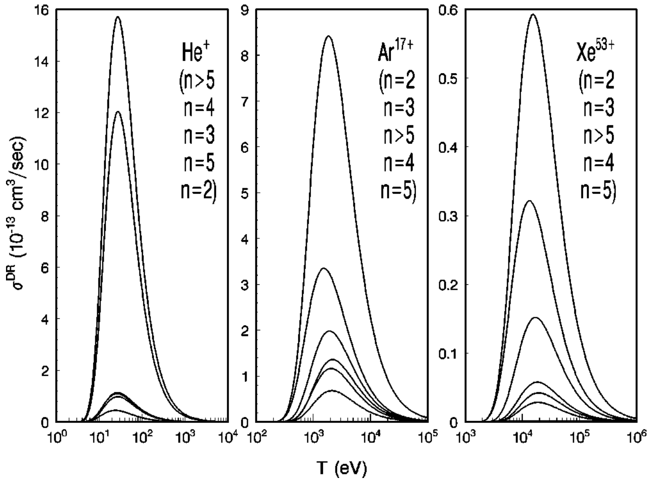

FIG. 3. The n dependence of the DR rate coefficients. The curves in the order from top to bottom are the total $2Lnl$ DR rate coefficients and partial rate coefficients as follows: (a) with $n>5$, $n=4,3,5,2$ for He^+; (b) with $n=2,3$, $n>5$, $n=4,5$ for Ar^{17+}; (c) with $n=2,3$, $n>5$, $n=4,5$ for Xe^{53+}.

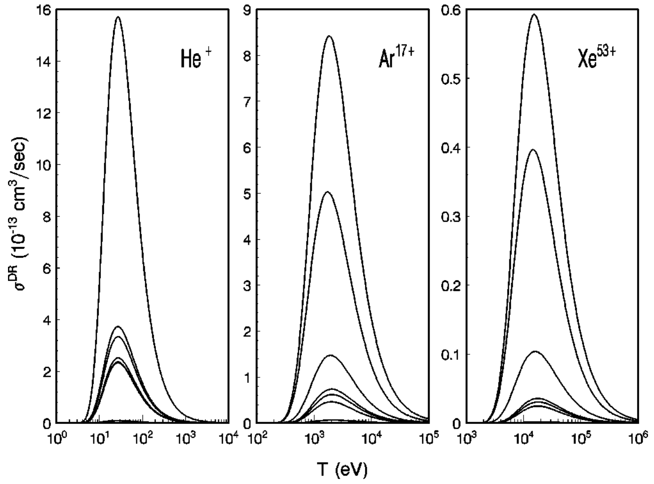

FIG. 4. The $\kappa(l)$ dependence of the DR rate coefficient. The curves in the order from top to bottom are the total $2Lnl$ DR rate coefficients and partial rate coefficients as follows: (a) with $l=p_{3/2},d_{5/2},s,d_{3/2},p_{1/2},f_{7/2},f_{5/2}$ for He^+; (b) with $l=p_{3/2},p_{1/2},d_{5/2},d_{3/2},s,f_{7/2},f_{5/2}$ for Ar^{17+}; (c) with $l=p_{3/2},p_{1/2},s,d_{5/2},d_{3/2},f_{7/2},f_{5/2}$ for Xe^{53+}.

The n dependence of the DR rate coefficients with $2Lnl$ intermediate states is shown in Fig. 3. The contribution of high-n doubly excited states ($n>5$) to α^{DR} is 87% for He^+, it decreases to 16% and 7% for Ar^{17+} and Xe^{53+}, respectively. Hence, the DR rate coefficients are dominated by the contribution of high-n states for low-Z ions and the low-n states for high-Z ions. This can be understood as follows. The radiative transition rates increase with Z rapidly (scaling as Z^4), while the Auger rates remain nearly the same (scaling as Z^0) [30]. For $Z\leqslant 20$, because the autoionizations are the dominant decay channels, $\Sigma_{k'}A^r_{jk'}\leqslant\Sigma_{i'}A^a_{ji'}$, $\alpha_{ij;k}\propto A^r_{jk}$, which depends on n very weakly, then the contribution of a large amount of high-n states is important. On the contrary, for high-Z ions, the radiative processes are the dominant decay channels, $\alpha_{ij;k}\propto A^a_{ij}\propto n^{-3}$ [30], the contribution of high-n states becomes less important. In the comparison with the absolute cross-section measurement [19], our calculated DR cross section of Ar^{17+} [17] is overestimated by about 10% for $n=2$, and underestimated by about 8% and 5% for $n=3,4$ double excited states, respectively. They are in general agreement with the experimental measurements for $n=5,6$. Thus, our calculated total DR cross section and rate coefficients for Ar^{17+} are anticipated to be larger and within about 8%. In Ref. [16], our calculated DR cross section of He^+ is overestimated by about 5% for $n=2$ and underestimated by about 5% for $n=3$, and slightly underestimated for $n=4$ and overestimated for $n=5$ double excited states compared with the measurements [18]. Thus, our calculated total DR cross section and rate coefficients for He^+ are anticipated to be larger and within about 6%. Figure 4 shows the $\kappa(l)$ dependence of the DR rate coefficients for He^+, Ar^{17+}, Xe^{53+}, and Au^{78+} ions with $2Lnl$ intermediate states. The DR rate coefficients is dominated by the contribution from the $l=1$ doubly excited states, and this contribution increase with the increase of Z.

In Table I, the peak values of the DR rate coefficients α^{DR}_{max} calculated by our SRCI method are compared with other theoretical works. In Ref. [31] Karim and Bhalla gave the DR rate coefficients for several hydrogenlike ions. In their calculation, α^{DR} were obtained explicitly in the nonrelativistic intermediate-coupling scheme including spin-orbit coupling for $n\leqslant 4$, for $n=5-8$ a configuration average scheme was used, and the n^{-3} scaling law was employed for $n\geqslant 9$. In Ref. [32] Karim and Ruesink recalculated α^{DR} for hydrogenlike ions with $Z=14$, 20, and 26, including the effect of configuration interaction and spin-orbit coupling for $n\leqslant 8$. The later results by Karim and Ruesink [32] are about 14% larger than the former ones by Karim and Bhalla [31]. Their new results [32] are still smaller than ours, while our results are closer to the results calculated by the Burgess formula [13], which is widely used for low-Z and intermediate-Z ions. In Nilson's work [33], the relativistic multiconfiguration wave functions are used and the n^{-3} scaling law is adopted to calculate the Auger rates for $n>4$ states, while we use the interpolation scheme based on QDT, which is more reasonable. For $Z=36,54$ (high Z) ions, where high-n double-excited states are not so important, his results of α^{DR}_{max} [33] agree with ours within 5%, and 2%, respec-

TABLE I. Comparison of theoretical α^{DR}_{max} of H-like ions.

		$\alpha^{DR}_{max}(10^{-13}$ cm^3/sec)			
Z	Ion	Our work	Burgess [1]	Karim [32]	Nilson [33]
2	He^+	17.9	19.9		
4	Be^{3+}	22.5	22.3		
10	Ne^{9+}	15.3	14.3		9.1
14	Si^{13+}	11.1	10.7	9.3	7.6
18	Ar^{17+}	8.7	8.4		6.1
20	Ca^{19+}	7.2	7.5	6.0	
26	Fe^{25+}	4.3	5.6	4.0	3.8
36	Kr^{35+}	1.9	3.5		1.8
54	Xe^{53+}	0.63	1.6		0.64
79	Au^{78+}	0.21	0.75		

tively. For low- and intermediate-Z ions, where high-n double-excited states are important, his results of $\alpha_{\max}^{\mathrm{DR}}$ [33] are significantly smaller than ours as shown in Table I. In Fig. 1, the total DR rate coefficients from the widely used Burgess formula [13] are compared with our SRCI results. The differences of $\alpha_{\max}^{\mathrm{DR}}$ between the two calculations are also shown in Table I. For He^{+} (low Z), the $\alpha_{\max}^{\mathrm{DR}}$ from the Burgess formula is about 11% larger than ours, which is anticipated to be 6% larger than the experimental rate coefficients [18] as discussed above. For the ions with intermediate Z $(10 \leqslant Z \leqslant 20)$, the $\alpha_{\max}^{\mathrm{DR}}$ calculated by the Burgess formula agree with ours within 7%, e.g., for Ar^{17+}, the $\alpha_{\max}^{\mathrm{DR}}$ from the Burgess formula is about 4% smaller than ours, which is anticipated to be 8% larger than the experimental rate coefficients [19]. The $\alpha_{\max}^{\mathrm{DR}}$ from the Burgess formula are significantly overestimated for high-Z atoms, e.g., 1.8, 2.5, and 3.5 times larger than our present calculations for Kr^{35+}, Xe^{53+}, and Au^{78+}, respectively. In this case, the relativistic effect should be considered. Thus, it can provide some clue about the validity of the Burgess formula from Table I. Because of its relativistic treatment, our SRCI method should be applicable for arbitrary Z ions and it can also be applied to the many-electron atoms, where the matrix elements have nodes.

ACKNOWLEDGMENTS

This work was partially supported by the Chinese Science and Technology Commission, the National High-Tech ICF Committee in China, the Science and Technology Funds of CAEP, the Chinese Research Association for Atomic and Molecular Data, and the Chinese NSF.

---

[1] A. Burgess, Astrophys. J. **139**, 776 (1964);

[2] A. V. Vinogradov, I. Yu. Skobelev, and E. A. Yukov, Zh. Eksp. Teor. Fiz. **72**, 1762 (1977) [Sov. Phys. JETP **45**, 925 (1977)].

[3] J. Dubau, A. H. Gabriel, M. Loulergue, L. Steenman-Clark, and S. Volone, Mon. Not. R. Astron. Soc. **195**, 705 (1981).

[4] W. Eissner and M. J. Seaton, J. Phys. B **6**, 2187 (1972).

[5] D. R. Flower and J. M. Launay, J. Phys. B **5**, L207 (1972).

[6] H. E. Saraph and M. J. Seaton, Philos. Trans. R. Soc. London, Ser. A **271**, 1 (1971).

[7] J. Dubau, Ph.D. thesis, University of London, 1973.

[8] Y. Hahn, Phys. Rev. A **22**, 2896 (1980).

[9] D. J. McLaughlin and Y. Hahn, Phys. Rev. A **29**, 712 (1984).

[10] M. H. Chen, Phys. Rev. A **31**, 1449 (1985).

[11] H. P. Saha, Phys. Rev. A **49**, 894 (1994).

[12] For example, M. H. Chen, Phys. Rev. A **33**, 994 (1986); J. Dubau, A. H. Gabriel, M. Loulergue, L. Steennan-Clark, and S. Volonte, Mon. Not. R. Astron. Soc. **195**, 705 (1981).

[13] A. Burgess, Astrophys. J. **141**, 1588 (1965).

[14] *Spectroscopy of Astrophysical Plasmas,* edited by A. Dalgarno and D. Layzer (Cambridge University Press, Cambridge, 1987).

[15] Chen-zhong Dong, Yu Zou, Jian-Guo Wang, and Jia-Ming Li, Acta Phys. Sin. **44**, 1712 (1995).

[16] Jian-Guo Wang, Yi-Zhi Qu, and Jia-Ming Li, Phys. Rev. A **52**, 4274 (1995).

[17] Jian-Guo Wang, Yu Zou, Chen-Zhong Dong, and Jia-Ming Li, Chin. Phys. Lett. **12**, 530 (1995).

[18] R. R. Harr, J. A. Tanis, V. L. Plano, K. E. Zaharakis, W. G. Graham, J. R. Mowat, T. Ellison, W. W. Jacobs, and T. Rinckel, Phys. Rev. A **47**, R3472 (1993).

[19] D. R. DeWitt, D. Schneider, M. W. Clark, and M. H. Chen, Phys. Rev. A **44**, 7185 (1991).

[20] Zhong-Xin Zhao and Jia-Ming Li, Acta Phys. Sin. **34**, 1469 (1985).

[21] Jia-Ming Li and Zhong-Xing Zhao, Acta Phys. Sin. **31**, 97 (1982).

[22] D. A. Liberman, D. T. Cromer, and J. T. Waber, Comput. Phys. Commun. **2**, 107 (1971).

[23] Lei Liu and Jia-Ming Li, Acta Phys. Sin. **42**, 1901 (1993).

[24] Jian-Guo Wang, Xiao-Ming Tong, and Jia-Ming Li, Acta Phys. Sin. **45**, 13 (1996); see also Yi-Zhi Qu, Jian-Guo Wang, and Jia-Ming Li, *ibid.* **46**, 249 (1997).

[25] For example, X. L. Liang and J. M. Li, Acta Phys. Sin. **34**, 1479 (1985); M. S. Wang and R. H. Pratt, Phys. Rev. A **29**, 174 (1984); R. Y. Yin and R. H. Pratt, *ibid.* **35**, 1154 (1987); X. M. Tong, L. Yang, and J. M. Li, Acta Phys. Sin. **38**, 407 (1989).

[26] C. M. Lee (Jia-Ming Li), Phys. Rev. A **10**, 584 (1974).

[27] K. R. Karim, Phys. Rev. A **43**, 615 (1991).

[28] D. R. DeWitt, E. Lindroth, R Schuch, H. Gao, T. Quinteros, and W. Zong, J. Phys. B **28**, L147 (1995).

[29] Jian-Guo Wang, Yi-Zhi Qu, Yu Zhou, Jun Yan, and Jia-Ming Li (unpublished).

[30] R. D. Cowan, *The Theory of Atomic Structure and Spectra* (University of California Press, Berkeley, 1981).

[31] K. R. Karim and C. P. Bhalla, Phys. Rev. A **37**, 2599 (1988).

[32] K. R. Karim and M. Ruesink, Phys. Rev. A **46**, 3904 (1992).

[33] J. Nilson, J. Quant. Spectrosc. Radiat. Transf. **36**, 539 (1986).

[34] Y. Hahn, Rep. Prog. Phys. **60**, 691 (1997).